

Supporting Information for

Quantitative insights into the mechanism of proton conduction and selectivity for the human voltage-gated proton channel Hv1

Yu Liu ^{†,a}, Chenghan Li ^{†,a}, Alfredo J. Freites ^b, Douglas J. Tobias ^b, Gregory A. Voth ^{a,1}

^aDepartment of Chemistry, Chicago Center for Theoretical Chemistry, Institute for Biophysical Dynamics and James Frank Institute, University of Chicago, Chicago, IL, 60637

^bDepartment of Chemistry, University of California, Irvine, CA 92697

¹Corresponding author: Gregory A. Voth
Email: gavoth@uchicago.edu

This PDF file includes:

- Supplementary Computational Details
- Supplementary Figures S1 to S4
- Supplementary Table S1
- SI References

Supplementary Computational Details

Transport rate constant calculations. The transport rate constant can be derived from the Nernst-Planck equation¹ in terms of the 1D free energy profile,

$$k = \frac{1}{\left(\int_{-z_0}^{z_0} d\Delta z \exp -\beta W(\Delta z) \right) \left(\int_{-z_0}^{z_0} d\Delta z \frac{\exp \beta W(\Delta z)}{D(\Delta z)} \right)} \quad (\text{S1})$$

where $W(\Delta z)$ is the 1D free energy profile (potential of mean force; PMF) of reaction coordinate Δz at value Δz , $D(\Delta z)$ is the ion position-dependent diffusion constant at Δz . Both $W(\Delta z)$ and $D(\Delta z)$ were computed from the equilibrium simulations without external electric field, which is a result of the fluctuation-dissipation theorem. The integral was performed over the transmembrane protein region defined as $-22 \text{ \AA} \leq \Delta z \leq +22 \text{ \AA}$.

Due to the exponential dependence on $W(z)$, the expression can be simplified as²

$$k = \frac{D(\Delta z_{TS})}{\left(\int_{-z_0}^{z_0} d\Delta z \exp -\beta W(\Delta z) \right) \left(\int_{-z_0}^{z_0} d\Delta z \exp \beta W(\Delta z) \right)} \quad (\text{S2})$$

where $D(\Delta z_{TS})$ is the diffusion constant calculated at the transition state of the system, corresponding to the top of the free energy barrier of the 1D PMF. The diffusion constant can be calculated as follows, according to Hummer, as³

$$D(\Delta z) = \frac{\text{Var}(\Delta z)^2}{\int_0^\infty dt C_{zz}(t)} \quad (\text{S3})$$

where $\text{Var}(\Delta z)$ stands for the variance of Δz , and $C_{zz}(t)$ is the time correlation function. $\text{Var}(\Delta z)$ and $C_{zz}(t)$ were computed from the z time series in the corresponding umbrella sampling window., and the time integral of $C_{zz}(t)$ was performed by first fitting to a triple exponential function, $a_1 \exp\left(-\frac{t}{t_1}\right) + a_2 \exp\left(-\frac{t}{t_2}\right) + a_3 \exp\left(-\frac{t}{t_3}\right)$, and then integrating it analytically.

In the case of proton permeation in the WT channel, the highest free energy point corresponds to the stage of proton freely diffusing in the bulk water. Thus, we took the experimental proton diffusion constant⁴ ($0.94 \text{ \AA}^2/\text{ps}$) in bulk water in the transport rate constant calculation for WT proton permeation process. We note that the proton diffusion constant in bulk directly obtained from MS-RMD⁵ is $0.37 \text{ \AA}^2/\text{ps}$, smaller than the experimental value. The discrepancy can be attributed to the missing nuclear quantum effects (NQE) in simulations with classical nuclei.⁶ In the D112N mutant, the transition state of the proton permeation corresponds to the excess proton staying on the first solvation shell of residue N112. We ran a separate MS-RMD simulation where an umbrella potential acted only on the reaction coordinate Δz_H with window center of value $\sim -1.0 \text{ \AA}$. The proton diffusion constant obtained from the simulation for D112N mutant at the transition ridge was $0.01 \text{ \AA}^2/\text{ps}$. The diffusion constant was corrected for the missing NQE by the ratio between experimental and the MS-RMD proton diffusion in bulk water and the corrected value was $0.03 \text{ \AA}^2/\text{ps}$.

The transport rate constant can also be computed from the transition matrix in the reaction coordinate space using a Markov state model (MSM) approach.⁷ The specific flavor of MSM we employed was the dynamic histogram analysis method (DHAM) framework,⁸ which relates the transition dynamics in biased simulations, such as umbrella sampling, to the unbiased transition

probability via a reweighting factor as a function of the bias potential. The proton permeation rate constant was computed to be the conditional reaction flux per unit time τ given that the proton had resided in the cytosolic bulk water last, given by

$$k^{\text{MSM}} = \frac{F}{\tau \sum_i \pi_i q_i^-} \quad (\text{S4})$$

The reaction flux for the entire proton permeation process was computed from the committor via

$$F = \sum_{i \in \text{Cytosol}} \sum_{j \in \text{Extracellular}} \pi_i P_{ij} q_j^+ \quad (\text{S5})$$

where π_i is the stationary probability of state i . The reactant state was defined as the transported proton inside cytosolic bulk water ($\Delta z_H \leq -22 \text{ \AA}$) and the product state was defined as the one inside extracellular bulk water ($\Delta z_H \geq 22 \text{ \AA}$).

The forward committor q_i^+ in the equations above determines^{9, 10, 11} the probability for the proton when currently being at state i will reach the extracellular bulk water next rather than return to the cytosol. The committor gradually increases its value from 0 to 1 from cytosolic bulk region to extracellular space and its value for intermediate states i ($-22 \text{ \AA} < \Delta z_H < 22 \text{ \AA}$) can be calculated from the transition matrix by solving the equations below¹²,

$$q_i^+ = \sum_{k \in \text{Intermediate}} P_{ik} q_k^+ + \sum_{k \in \text{Extracellular}} P_{ik} \quad (\text{S6})$$

where P_{ik} is the transition matrix element, indicating the transition probability from state i to state k within lag time τ . At equilibrium, the backward committor can be calculated as $q_i^- = 1 - q_i^+$. The umbrella sampling trajectories were partitioned into 6 equally sized blocks and the MSM rate standard error was calculated using the last 5 blocks out of 6. Results are in Table S1. Figure S4 shows the saturated rate constant as a function of increasing lag time.

Maximum conductance calculation. The unitary maximum conductance g_1^{max} was calculated from transport rate constant k_1 via^{13, 14}

$$g_1^{\text{max}} = \frac{k_1 q^2}{k_B T} \quad (\text{S7})$$

where q is the charge of the transported ion, k_B is Boltzmann's constant, and T is the temperature in Kelvin (300 K for our system).

Supplementary Figures

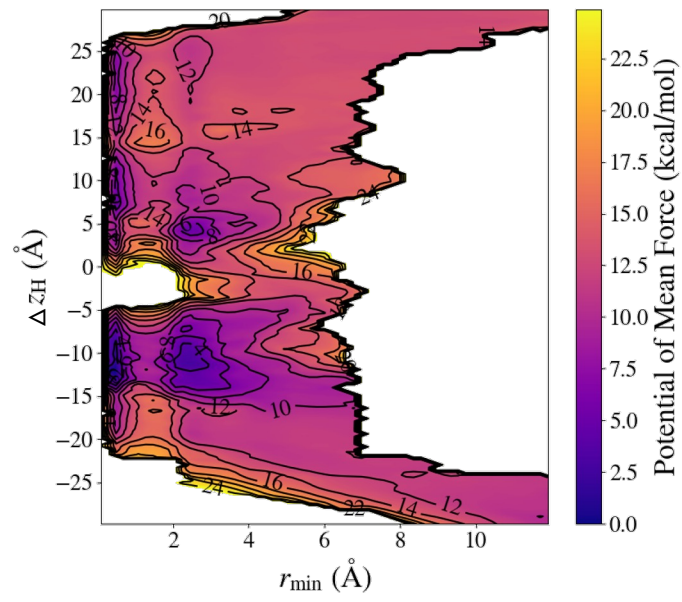


Figure S1. Excess proton 2D PMF in the D112N mutant.

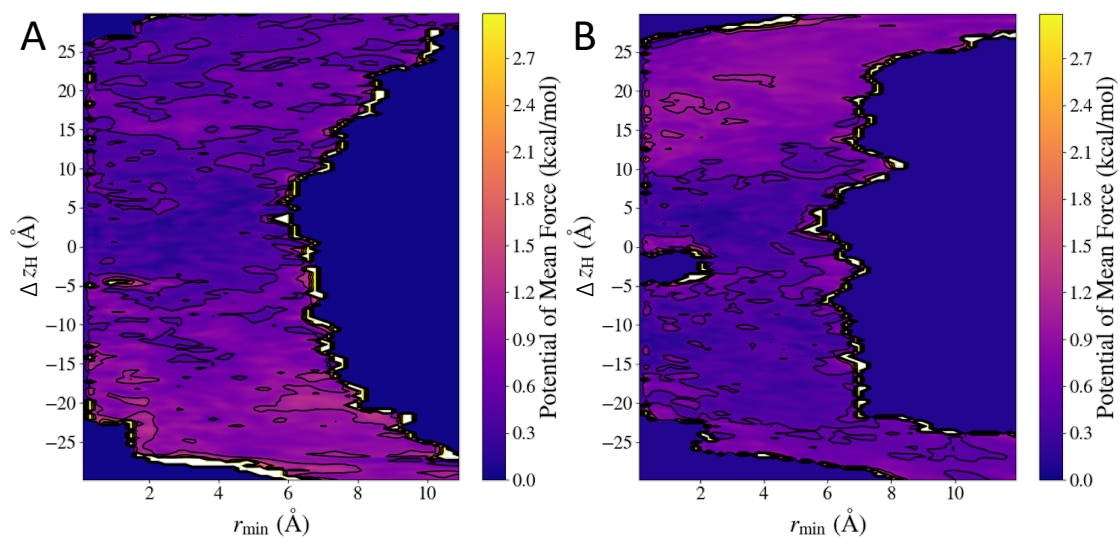


Figure S2. Proton 2D PMF error profiles. Panel A) WT. Panel B) D112N mutant. The standard deviation was calculated by aligning the 2D PMF of each block by setting the total probability of the 2D PMF to 1.

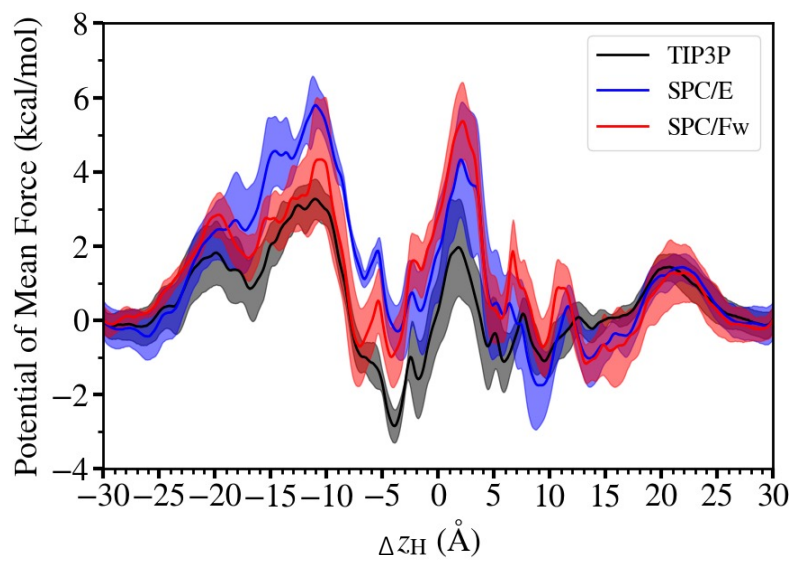


Figure S3. TMA+ PMF with different water models: TIP3P, SPC/E SPC/Fw.

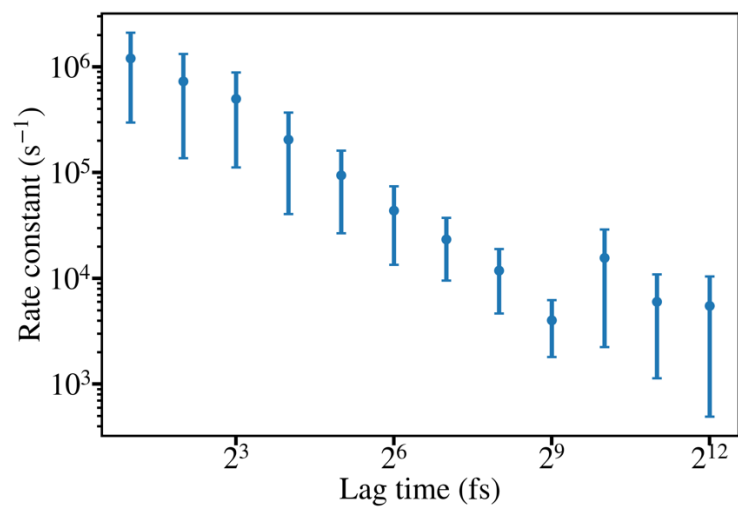


Figure S4. Rate constant calculated from the MSM with different lag times for proton permeation in WT hHv1. The rate constant value calculated from Nernst-Planck equation with diffusion constant is $(3.5 \pm 0.7) \times 10^3 \text{s}^{-1}$, which is in good agreement with the MSM estimated rate constant $(4.0 \pm 2.2) \times 10^3 \text{s}^{-1}$ from a lag time of 0.5 ps.

Supplementary Table S1. Diffusion constant calculated from classical ion permeation. *

WT hHv1	Diffusion constant ($\text{\AA}^2/\text{ps}$)	D112N mutant	Diffusion constant ($\text{\AA}^2/\text{ps}$)
TMA ⁺	0.004 (0.002 to 0.004)	TMA ⁺	0.004 (0.003 to 0.006)
CH ₃ SO ₃ ⁻	0.002 (0.001 to 0.002)	CH ₃ SO ₃ ⁻	0.002 (0.002 to 0.006)

*The diffusion constants were calculated from umbrella window trajectories corresponding to the transition state position in the 1D PMF of ion permeation process. The experimental TMA⁺ diffusion constant¹⁵ in bulk water is 0.093 $\text{\AA}^2/\text{ps}$. The value in the parenthesis represents the range of the diffusion constant of the reaction coordinate $\pm 0.5 \text{\AA}$ adjacent to the transition state.

SI References

1. Levitt DG. Interpretation of biological ion channel flux data—reaction-rate versus continuum theory. *Annual review of biophysics and biophysical chemistry* **15**, 29-57 (1986).
2. Woolf TB, Roux B. Conformational flexibility of o-phosphorylcholine and o-phosphorylethanolamine: a molecular dynamics study of solvation effects. *Journal of the American Chemical Society* **116**, 5916-5926 (1994).
3. Hummer G. Position-dependent diffusion coefficients and free energies from Bayesian analysis of equilibrium and replica molecular dynamics simulations. *New Journal of Physics* **7**, 34 (2005).
4. Roberts NK, Northey HL. Proton and deuteron mobility in normal and heavy water solutions of electrolytes. *Journal of the Chemical Society, Faraday Transactions 1: Physical Chemistry in Condensed Phases* **70**, 253-262 (1974).
5. Biswas R, Tse Y-LS, Tokmakoff A, Voth GA. Role of presolvation and anharmonicity in aqueous phase hydrated proton solvation and transport. *The Journal of Physical Chemistry B* **120**, 1793-1804 (2016).
6. Calio PB, Li C, Voth GA. Resolving the Structural Debate for the Hydrated Excess Proton in Water. *Journal of the American Chemical Society* **143**, 18672-18683 (2021).
7. Suárez E, Wiewiora RP, Wehmeyer C, Noé F, Chodera JD, Zuckerman DM. What Markov state models can and cannot do: Correlation versus path-based observables in protein-folding models. *Journal of chemical theory and computation* **17**, 3119-3133 (2021).
8. Rosta E, Hummer G. Free energies from dynamic weighted histogram analysis using unbiased Markov state model. *Journal of chemical theory and computation* **11**, 276-285 (2015).
9. Vanden-Eijnden E. Towards a theory of transition paths. *Journal of statistical physics* **123**, 503-523 (2006).
10. Du R, Pande VS, Grosberg AY, Tanaka T, Shakhnovich ES. On the transition coordinate for protein folding. *The Journal of chemical physics* **108**, 334-350 (1998).
11. Bolhuis PG, Chandler D, Dellago C, Geissler PL. Transition path sampling: Throwing ropes over rough mountain passes, in the dark. *Annual review of physical chemistry* **53**, 291-318 (2002).
12. Noé F, Schütte C, Vanden-Eijnden E, Reich L, Weikl TR. Constructing the equilibrium ensemble of folding pathways from short off-equilibrium simulations. *Proceedings of the National Academy of Sciences* **106**, 19011-19016 (2009).
13. Roux B, Allen T, Berneche S, Im W. Theoretical and computational models of biological ion channels. *Quarterly reviews of biophysics* **37**, 15-103 (2004).

14. Zhekova HR, Ngo V, da Silva MC, Salahub D, Noskov S. Selective ion binding and transport by membrane proteins—A computational perspective. *Coordination Chemistry Reviews* **345**, 108-136 (2017).
15. Eriksson P-O, Lindblom G, Burnell EE, Tiddy GJT. Influence of organic solutes on the self-diffusion of water as studied by nuclear magnetic resonance spectroscopy. *Journal of the Chemical Society, Faraday Transactions 1: Physical Chemistry in Condensed Phases* **84**, 3129-3139 (1988).